MGCD0103, a novel isotype-selective histone deacetylase inhibitor, has broad spectrum antitumor activity *in vitro* and *in vivo*

Marielle Fournel,[1] Claire Bonfils,[1] Yu Hou,[1] Pu Theresa Yan,[1] Marie-Claude Trachy-Bourget,[1] Ann Kalita,[1] Jianhong Liu,[1] Ai-Hua Lu,[2] Nancy Z. Zhou,[3] Marie-France Robert,[4] Jeffrey Gillespie,[5] James J. Wang,[5] Hélène Ste-Croix,[4] Jubrail Rahil,[2] Sylvain Lefebvre,[4] Oscar Moradei,[3] Daniel Delorme,[3] A. Robert MacLeod,[4] Jeffrey M. Besterman,[1,2,3,4,5] and Zuomei Li[1]

Departments of [1]Molecular Biology, [2]Lead Discovery, [3]Medicinal Chemistry, [4]Cell Biology and Pharmacology, and [5]Pharmacokinetics, MethylGene, Inc., St. Laurent, Quebec, Canada

Abstract

Nonselective inhibitors of human histone deacetylases (HDAC) are known to have antitumor activity in mice *in vivo*, and several of them are under clinical investigation. The first of these, Vorinostat (SAHA), has been approved for treatment of cutaneous T-cell lymphoma. Questions remain concerning which HDAC isotype(s) are the best to target for anticancer activity and whether increased efficacy and safety will result with an isotype-selective HDAC inhibitor. We have developed an isotype-selective HDAC inhibitor, MGCD0103, which potently targets human HDAC1 but also has inhibitory activity against HDAC2, HDAC3, and HDAC11 *in vitro*. In intact cells, MGCD0103 inhibited only a fraction of the total HDAC activity and showed long-lasting inhibitory activity even upon drug removal. MGCD0103 induced hyperacetylation of histones, selectively induced apoptosis, and caused cell cycle blockade in various human cancer cell lines in a dose-dependent manner. MGCD0103 exhibited potent and selective antiproliferative activities against a broad spectrum of human cancer cell lines *in vitro*, and HDAC inhibitory activity was required for these effects. *In vivo*, MGCD0103 significantly inhibited growth of human tumor xenografts in nude mice in a dose-dependent manner and the antitumor activity correlated with induction of histone acetylation in tumors. Our findings suggest that the isotype-selective HDAC inhibition by MGCD0103 is sufficient for antitumor activity *in vivo* and that further clinical investigation is warranted. [Mol Cancer Ther 2008;7(4):759–68]

Received 8/30/07; revised 12/20/07; accepted 1/21/08.

The costs of publication of this article were defrayed in part by the payment of page charges. This article must therefore be hereby marked *advertisement* in accordance with 18 U.S.C. Section 1734 solely to indicate this fact.

Note: M. Fournel and C. Bonfils contributed equally to this paper.

Current address for D. Delorme: Neurochem, Inc., 275 Armand-Frappier Boulevard, Laval, Quebec H7V 4A7, Canada.

Current address for A.R. MacLeod: Takeda San Diego, Inc., 10410 Science Center Drive, San Diego, CA 92121, USA.

Requests for reprints: Zuomei Li, Department of Molecular Biology, MethylGene, Inc., 7220 Frederick-Banting, Montreal, Quebec H4S 2A1, Canada. Phone: 514-337-3333, ext. 245; Fax: 514-337-0550. E-mail: liz@methylgene.com

doi:10.1158/1535-7163.MCT-07-2026

Introduction

Histone deacetylases (HDACs) are a family of enzymes which deacetylate lysines on core histones and other cellular proteins (1, 2). They play an important role in epigenetic regulation of gene transcription and also control other cellular functions, such as proliferation, cell death, and motility (2). There are currently 18 known mammalian deacetylase enzymes which can be divided into two major groups: Zn^{2+}-dependent HDACs (1, 2) and NAD^{+}-dependent sirtuins (3, 4). Zn^{2+}-dependent HDACs can be further subdivided into three classes: class I, which is homologous to yeast Rpd3, includes HDAC1 (5), HDAC2 (6), HDAC3 (7), and HDAC8 (8, 9); class II, which shows homology to yeast Hda1, includes HDAC4, HDAC5, HDAC6, HDAC7, HDAC9, and HDAC10 (10–15); and HDAC11 (16) is the sole member of class IV HDACs. Sirtuins are designated as class III deacetylases.

In human cancer cells, loss of acetylation on H4 histones is associated with early tumorigenesis (17). Overexpression of HDAC enzymes is observed in various primary human cancer tissues, including stomach, colon, breast, and prostate (18–22). In human leukemic cells, dysregulation of HDAC activity by chromosome translocation has been observed (23, 24). Inhibitors of HDAC enzymes are emerging as new targets for cancer therapy in recent years (25–31).

HDAC inhibitors under clinical investigation differ in chemical classes (for recent reviews, see refs. 27, 28, 30). The nonselective HDAC inhibitors, which have nanomolar and submicromolar IC_{50}s, include hydroxamic acid inhibitors, such as SAHA (Vorinostat; ref. 32), LBH589 (Panobinostat; ref. 33), and PXD101 (Belinostat; ref. 34), or cyclic tetrapeptides (Romidepsin or depsipeptide/FR901228; ref. 35). Among them, SAHA (Vorinostat) was recently approved in the United States for patients with cutaneous T-cell lymphoma who have progressive, persistent, or recurrent disease (36). A benzamide HDAC inhibitor, MS-275 (Syndax; ref. 37), is reported to be a selective HDAC inhibitor targeting class I HDACs (38).

As the efficacy and safety data from human cancer trials with nonselective HDAC inhibitors emerge, the question remains as to whether it will be advantageous to develop isotype-selective inhibitors to improve the therapeutic index over non-selective inhibitors (39). Additionally, research continues to define which specific HDAC isotype(s) are better targets for human cancer therapy. In this report, we show that selective HDAC1 inhibition leads to apoptosis and growth arrest of human cancer cells *in vitro* and that isotype-selective inhibition of HDAC enzymes by MGCD0103 is sufficient for antitumor activity in a broad spectrum of human cancer cells, both *in vitro* and *in vivo*.

Materials and Methods

Chemicals

MGCD0103, *N*-(2-amino-phenyl)-4-((4-pyridin-3-yl-pyrimidin-2-ylamino)-methyl)-benzamide (dihydrobromide salt), and its inactive desamino analogue, compound A (*N*-phenyl-4-((4-(pyridin-3-yl)pyrimidin-2-ylamino)methyl)benzamide) were designed and synthesized in-house. In all *in vitro* assays and *in vivo* analyses, the free base version of MGCD0103 was used, except where indicated. All other comparator HDAC inhibitors used were also synthesized in-house. Other chemicals used were purchased from Sigma-Aldrich, except where indicated.

Cell Culture

Human mammary epithelial cells (HMEC) and human foreskin fibroblasts (MRHF) were obtained from BioWhittaker. All other cell lines were from American Type Culture Collection. All cells were cultured following the vendor's instructions.

Antisense Oligos of Human HDAC Isotypes

Antisense oligo-deoxyribonucleotides (oligos) were synthesized with the phosphorothioate backbone and the 4×4 nucleotides 2′-*O*-methyl modification on an automated synthesizer and purified by preparative reverse-phase high-performance liquid chromatography. All oligos were 20 bases in length, targeting sequences in the 5′ or 3′ untranslated regions of *HDAC* genes. Oligos were used at various doses to transfect human non–small cell lung cancer (NSCLC) A549 cells or human bladder T24 cells for 4 h with Lipofectin (Life Technologies Invitrogen) following manufacturer's instructions. Active oligos against specific *HDAC* isotypes were identified by analyzing target gene expression at the mRNA level (Northern blotting) 24 h after transfection. The sequences of the active antisense oligos used in this study, targeting human *HDAC1, HDAC2, HDAC3,* and *HDAC6*, as well as the corresponding mismatch oligos, are listed under Supplementary Materials.

Production of Recombinant HDAC Enzymes

cDNAs of human *HDAC1* to *HDAC8* and *HDAC11* were generated by reverse transcription–PCR reactions using primers complementary to the 5′ and 3′ coding sequence of human HDAC gene sequences in Genbank. cDNAs corresponding to the full-length human *HDAC1, HDAC2, HDAC3,* and *HDAC11* were cloned into pBlueBac4.5 vector (Invitrogen). The constructs were used to generate recombinant baculoviruses using the Bac-N-Blue DNA according to the manufacturer's instructions (Invitrogen). The recombinant HDAC1, HDAC2, HDAC3, HDAC11 proteins produced harbor a FLAG tag at their COOH termini. cDNAs encoding truncated versions of HDAC4, HDAC5, and HDAC7 encompassing their deacetylase domains were cloned into pDEST10 as an NH_2 terminal hexahistidine fusion protein and recombinant baculoviruses were generated using the Bac-to-Bac baculovirus expression system (Invitrogen). *HDAC6* and *HDAC8* were cloned as full-length NH_2 terminally His-tagged proteins. All HDAC proteins were expressed in insect Sf-9 cells (*Spodoptera frugiperda*) upon infection with recombinant baculovirus. HDAC1 enzyme was purified from the Q-sepharose FF column (Amersham Pharmacia Biotech) followed by an anti-FLAG immunoaffinity column (Sigma). HDAC2, HDAC3, and HDAC11 were purified using Flag-antibody immunoaffinity purification. HDAC4, HDAC5, HDAC6, HDAC7, and HDAC8 were purified using either Ni-NTA resin (QIAGEN) or His-Select resin (Sigma) with step washes and elution with different concentrations of imidazole in Buffer containing 25 mmol/L Tris (or $NaPO_4$; pH 8.0), 10% glycerol, and 150 mmol/L or 500 mmol/L NaCl.

HDAC Enzyme Assay *In vitro*

The deacetylase enzyme assay was based on a homogeneous fluorescence release assay. Purified recombinant HDAC enzymes were incubated with compounds diluted in various concentrations for 10 min in assay buffer [25 mmol/L HEPES (pH 8.0), 137 mmol/L NaCl, 1 mmol/L $MgCl_2$, 2.7 mmol/L KCl] at room temperature. The substrate Boc-Lys(ε-Ac)-AMC (Bachem) was added to the reaction for further incubation at 37°C. The concentration of the substrate and the incubation time varied for different isotypes of HDAC enzymes. A 20-min trypsin incubation at room temperature allowed the release of the fluorophore from the deacetylated substrate. The fluorescent signal was detected by fluorometer (Molecular Devices; GeminiXS) at excitation of 360 nm, emission of 470 nm, and cutoff at 435 nm. The IC_{50} values of the compounds were determined by analyzing dose-response inhibition curves.

HDAC Whole-Cell Assay

Cells were seeded into 96-well plates (Corning, Inc.; Costar) at an appropriate density (human colon cancer HCT116 and HCT15 cells, 1×10^5 per well; human prostate cancer DU145 and human NSCLC A549 cells, 5×10^4 per well) in a volume of 50 μL of appropriate tissue culture medium. Compounds were added at desired concentrations for the indicated length of incubation at 37°C with 5% CO_2. To initiate the reaction, Boc-Lys(ε-Ac)-AMC (Bachem; I-1875) was added to a final concentration of 300 μmol/L. The reaction was stopped after 90 min, and fluorescence was developed by adding 50 μL of freshly prepared stop mix: Fluor-de-Lys developer diluted at 1:60 (BioMol), 1 μmol/L TSA (BioMol), 1% NP40. All components of the stop mix were diluted in HDAC assay buffer [25 mmol/L Tris-HCl (pH 8.0), 137 mmol/L NaCl, 2.7 mmol/L KCl, 1 mmol/L $MgCl_2$]. The reaction was allowed to develop for

at least 15 min at 37°C, and the fluorescent signal was detected by fluorometry (Molecular Devices; GeminiXS) at excitation of 360 nm, emission of 470 nm, and cutoff at 435 nm. A standard curve with known amounts of Boc-Lys-AMC (Bachem) was used to convert the fluorescence readings into micromolar product.

Western Blot Analysis

Whole-cell extracts were generated from cell pellets lysed in buffer [25 mmol/L Tris-HCl (pH 7.5), 1 % Triton X-100, 0.5% Na-deoxycholate, 5 mmol/L EDTA] supplemented with protease inhibitors (1 μg/mL pepstatin, 2 μg/mL leupeptin, 2 μg/mL aprotinin, 5 μg/mL TLCK, 5 μg/mL phenylmethylsulfonyl fluoride), 5 μg/mL DTT, and 5 mmol/L sodium butyrate. Histones were extracted as described (40). Proteins were transferred onto a polyvinylidene difluoride membrane and probed with either HDAC1 (Santa Cruz Biotechnology), HDAC2 (Santa Cruz Biotechnology), HDAC3 (Sigma), HDAC6 (in-house), acetylated H4 (Upstate Biotechnology, Inc.), acetylated H3 (Upstate Biotechnology, Inc.), total histone H3 (Abcam), PARPcssa (Biosource, Medicorp), $p21^{WAF1/Cip1}$ (Transduction Laboratories), tubulin (Sigma), actin (Santa Cruz Biotechnology), or glyceraldehyde-3-phosphate dehydrogenase (Ambion, Inc.). Horseradish peroxidase–conjugated secondary antibodies (Sigma) were used with enhanced chemiluminescence (Amersham Pharmacia Biotech) for detection.

Flow Cytometric Cell Cycle Analysis

Cells were treated with inhibitors for 16 h, harvested, and fixed with 70% ethanol at −20°C. Nucleic acids from fixed cells were treated with RNase type III A (1 mg/mL) and stained with propidium iodide (50 μg/mL). DNA content was measured by using a fluorescence-activated cell cytometer (FACScan, Becton Dickinson) and analyzed using CellQuest Pro software.

Cell Viability Assay

Cells in 96-well plates were incubated with compounds at various concentrations for 72 h at 37°C in 5% CO_2. 3-(4,5-Dimethylthiazol-2-yl)-2,5-diphenyltetrazolium bromide (MTT; Sigma) was added at a final concentration of 0.5 mg/mL and incubated with the cells for 4 h before an equal volume of solubilization buffer [50% *N*,*N*-dimethylformamide, 20% SDS (pH 4.7)] was added. After overnight incubation, solubilized dye was quantified by reading at 570 nm using a reference at 630 nm. Absorbance values were converted to cell numbers according to a standard growth curve of the relevant cell line. The concentration which reduced cell numbers to 50% relative to DMSO-treated cells was determined as MTT IC_{50}.

Detection of Apoptosis

Cells were transfected with antisense oligonucleotides for 4 h everyday for 2 d. At 48 h after initial transfection, cells were harvested and apoptosis was evaluated with the Cell Death Detection ELISA Plus kit (Roche) following manufacturer's protocol. In all experiments, a fixed amount of DNA-histone complex, provided with the ELISA kit as a positive control, was used to ensure results were comparable among experiments. To analyze caspase-dependent apoptosis, an antibody specifically recognizing the caspase cleavage fragment of human poly(ADP-ribose) polymerase (PARP; BioSource) was used to probe Western blots of lysates from cells treated with MGCD0103.

In vivo Antitumor Efficacy and Drug Pharmacokinetic Studies

Female CD-1 nude mice, ages 8 to 10 wk (Charles River Laboratories), were used. Tumor fragments (~30 mg), which had been serially passaged thrice *in vivo* in minimal, were implanted s.c. through a small surgical incision on the flank of the mice while under general anesthesia. HDAC inhibitors were dissolved in vehicle (PBS acidified with 0.1 N HCl or PEG400/0.2 N HCl saline, 40:60) and dosed p.o. as solutions daily. Tumor volumes and body weight were monitored thrice weekly for at least 2 wk. Each experimental group contained six to eight animals. For pharmacokinetic study, blood was collected from animals at various time points, and plasma samples were analyzed using an Agilent 1100 HPLC system coupled with an MDS Sciex API2000 triple quadrupole mass spectrometer.

Statistical Analysis

The terminal tumor volumes from *in vivo* xenograft studies were subjected to one-way ANOVA analysis followed by Dunnett's test when there were multiple treatment groups. For experiments where only vehicle group and a single treatment group were compared, Student's *t* test was used. Results were considered statistically significant when $P < 0.05$.

Results

Isotype-Specific Antisense Inhibition of HDAC1 in Human Cancer Cells Selectively Blocks Proliferation of Human Cancer Cells and Induces Apoptosis

Isotype-selective antisense inhibitors depleted corresponding target HDACs at both mRNA and protein levels in a dose-dependent and time-dependent manner (data not shown). As shown in Fig. 1A, specific depletion of HDAC1, HDAC2, HDAC3, and HDAC6 at the protein level was achieved in human NSCLC A549 cells.

In multiple independent experiments, we analyzed apoptosis or proliferation of A549 cells ($n = 6$) and HMEC cells ($n = 3$) treated with antisense inhibitors to HDAC1, HDAC2, HDAC3, and HDAC6 (Fig. 1B and C). As shown in Fig. 1B as a typical experiment, HDAC1 antisense, but not antisense to other isotypes or a mismatch control, induced apoptosis of A549 cells. The HDAC1 antisense did not result in apoptosis of normal HMEC cells (Fig. 1C), although target inhibition was equally achieved in both A549 and HMEC cells (data not shown). In addition to inducing apoptosis, HDAC1 antisense, but not the other antisense, significantly blocked proliferation of A549 cells *in vitro* in a dose-dependent manner (Fig. 1D). The antiproliferative effect from HDAC1 inhibition was also observed in four other human cancer cell lines from various tissue origins, including bladder T24, colorectal HCT116, prostate Du145, and breast MCF7 cancer cell lines (data not shown).

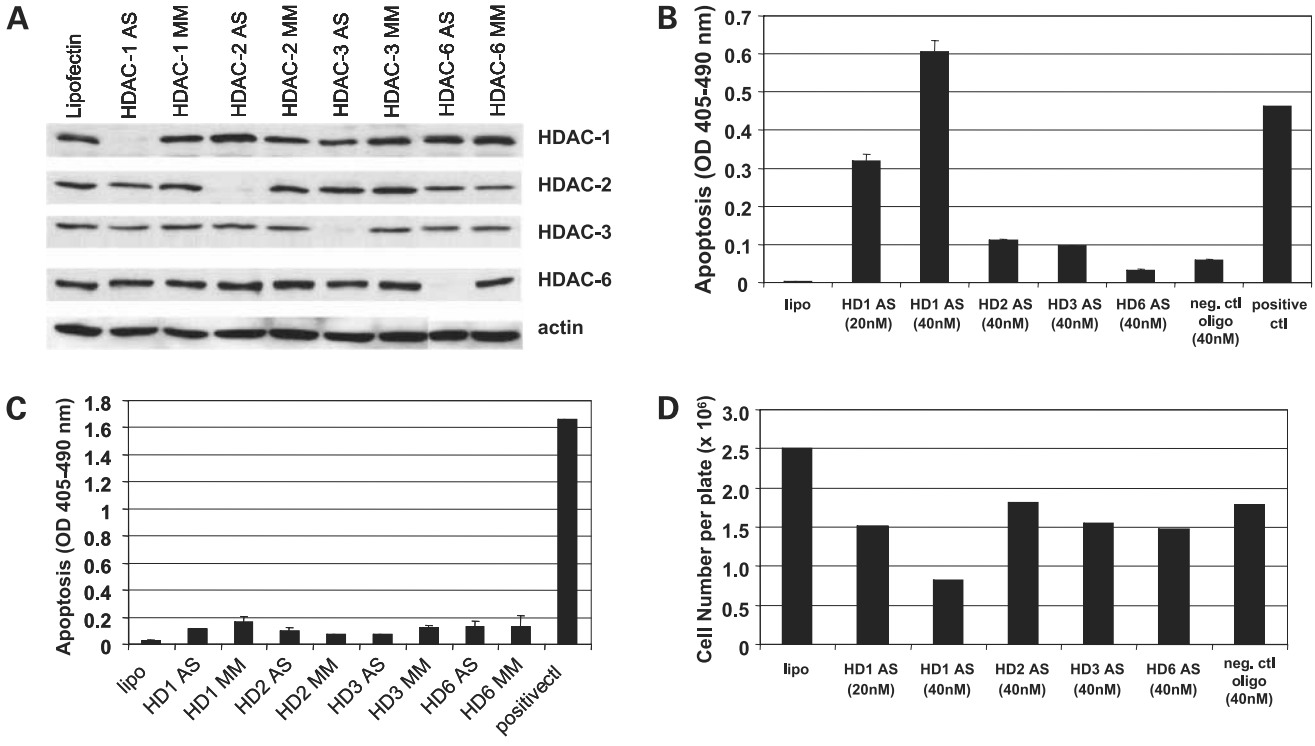

Figure 1. **A,** isotype-selective antisense oligonucleotides specifically knocked down target HDAC isotypes in A549 human NSCLC cells. Cells were treated with HDAC isotype-selective antisense inhibitors at 50 nmol/L, and treatment was repeated every 24 h for 72 h. The expression levels of HDAC1, HDAC2, HDAC3, and HDAC6 were detected by Western blot analysis. **B,** specific inhibition of HDAC1 (but not HDAC2, HDAC3, and HDAC6) by antisense inhibitor induced apoptosis in A549 cells *in vitro*. Cells were treated with isotype-selective antisense inhibitors every 24 h for 48 h. Apoptosis was detected as nucleosome release with Cell Death Detection ELISA Plus kit (Roche). Positive control is a DNA-histone complex provided with the ELISA kit, serving as an assay control and normalization control between independent experiments. Negative control is a mixture of 20-mer random sequence oligos, with all deoxyribonucleotides (A, T, G, and C) being represented in equimolarity at any position. *Lipo,* Lipofectin control with no oligo. The final concentration of oligos was fixed to 40 nmol/L for all conditions, except for the Lipofectin control; when HDAC1 antisense was evaluated at 20 nmol/L, it was supplemented with 20 nmol/L of the negative control oligo to bring the final concentration to 40 nmol/L. **C,** HDAC antisense inhibitors did not induce apoptosis in normal HMEC. Cells were treated with 50 nmol/L of isotype-selective antisense inhibitors every 24 h for 72 h. The same detection method as for **B** was applied to assess the levels of apoptosis. **D,** specific inhibition of HDAC1 by antisense inhibitor induced growth arrest in A549 cells *in vitro*. This is the same experiment as **B**. Before cells were evaluated for apoptosis, they were counted by trypan blue exclusion.

MGCD0103 Is an Isotype-Selective HDAC Inhibitor *In vitro*

As shown in Table 1, MGCD0103 inhibited only a subset of the nine human recombinant HDACs, including HDAC1, HDAC2, HDAC3, and HDAC11 at nanomolar or low micromolar concentrations, in a dose-dependent manner. MGCD0103 exhibited most potent inhibitory activity against human HDAC1 and HDAC2 enzymes *in vitro*, and it did not inhibit class II HDACs. The exocyclic amino group in MGCD0103 was necessary for

Table 1. Structures and IC_{50}s of MGCD0103 and its inactive analogue (compound A) against recombinant human HDACs

	Structure	Compound IC_{50} ± SE (μmol/L)*								
		HD1	HD2	HD3	HD4	HD5	HD6	HD7	HD8	HD11
MGCD0103	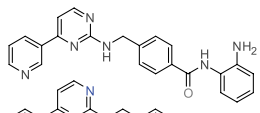	0.15 ± 0.02	0.29 ± 0.08	1.66 ± 0.69	>10	>10	>10	>10	>10	0.59 ± 0.23
Compound A	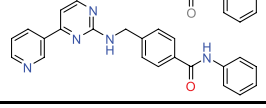	>10	>10	N.E.	>10	>10	>10	>10	>10	N.E.

Abbreviation: N.E., not evaluated.

*IC_{50} is the concentration that reduces initial activity to 50%. IC_{50} >10 μmol/L means there was no significant inhibition in two independent dose-response analyses of up to 10 μmol/L; other IC_{50}s were determined from 6 to 21 independent experiments.

enzyme inhibitory activity because HDAC-inhibitory activity against HDAC1 and HDAC2 was completely abolished with the desamino analogue (compound A, Table 1).

Whole-Cell Inhibitory Activity of MGCD0103 and Other HDAC Inhibitors in Human Cancer Cells

The whole-cell HDAC enzyme inhibitory activity of MGCD0103 was compared with other HDAC inhibitors. As shown in Fig. 2A, the inhibitory activity of MGCD0103 reached the maximum plateau at 6 μmol/L, and the maximal inhibitable enzyme pool affected by MGCD0103 was 75% of the total enzyme activity in HCT116 cells whereas NVP-LAQ824 inhibited almost 100% of that in these cells. We also analyzed dose-dependent inhibitory activity of MGCD0103 in other human tumor cells, including DU145, HCT15 (Fig. 2B), A549, T24, MCF-7, Panc1, and U87-MG (data not shown). In all cell lines tested, MGCD0103 partially inhibited cellular HDAC enzyme activity although the maximal inhibition of activity varied among cell lines from 75% to 85% of total activity. The IC_{50} of MGCD0103 in intact cancer cells was independent of tissue origin. The inactive analogue of MGCD0103, compound A, did not have HDAC inhibitory activity in whole cells (Fig. 2B). SAHA was tested in several cancer cell lines (e.g., HCT116, DU145, A549 cells) in multiple independent experiments and was consistently found to be a weaker inhibitor than MGCD0103 despite inhibition of a larger percentage of total cellular HDAC activity (Fig. 2B).

Persistence of MGCD0103 Inhibitory Activity in Whole Cells

In A549 cells, both MGCD0103 and SAHA showed dose-dependent inhibition of HDAC activity in whole cells (Fig. 2C). At high concentrations in A549 cells, SAHA inhibited >90% of total HDAC activity whereas MGCD0103 inhibited a maximum of 80% of total activity. Cells were then subsequently washed with drug-free media. As shown in Fig. 2C, the inhibitory activity of SAHA was almost completely reversed during the HDAC whole-cell activity assay immediately after drug wash-off. However, the inhibitory activity of MGCD0103 was sustained at least

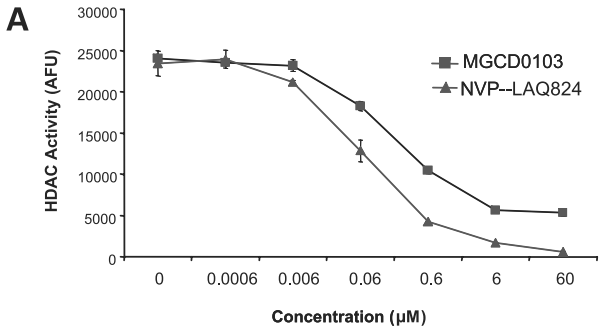

B

	n	Du145	n	HCT15	n	HCT116
MGCD0103	10	0.45+/–0.04	6	0.45+/–0.01	8	0.45+/–0.02
SAHA	4	0.72+/–0.03	4	0.83+/–0.06	5	2.98+/–0.09
Compound A	3	>50	3	>50	3	>50

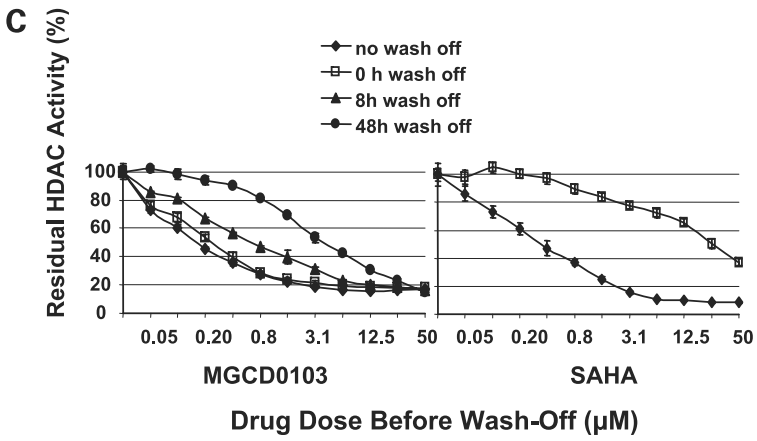

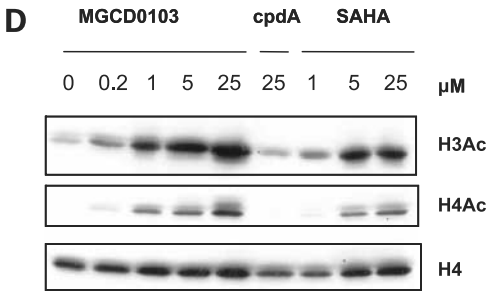

Figure 2. Pharmacologic effects of MGCD0103 in human cancer cells *in vitro*. **A,** dose-dependent inhibition of whole-cell HDAC activity in cultured HCT116 human colon cancer cells by MGCD0103 (*squares*) and NVP-LAQ824 (*triangles*). Cells were incubated with inhibitors for 24 h before whole-cell HDAC enzyme activity assay was performed. **B,** IC_{50}s (μmol/L ± SE) of whole-cell HDAC inhibition by MGCD0103, SAHA, and compound A in various human cancer cell lines. Cells were incubated with inhibitors for 24 h before enzyme activity was analyzed. **C,** whole-cell HDAC inhibitory activity of SAHA and MGCD0103 in wash-off experiment in A549 cells. Cells were treated with inhibitors at various doses for 16 h. The inhibitors were washed off with PBS and fresh drug-free medium was added. The whole-cell HDAC activity was assayed for 1 h, starting at indicated time points: no wash-off (*diamond*), immediately after wash-off (0 h; *open square*), 8 h after wash-off (*triangle*), 48 h after wash-off (*circle*). HDAC activity in cells 8 h and 48 h after wash-off following treatment with SAHA has also been analyzed (not shown) and was identical to the activity measured immediately after wash-off (0 h). **D,** dose-dependent induction of histone acetylation *in vitro* in T24 human bladder cancer cells by MGCD0103, compound A, and SAHA. Cells were incubated with inhibitors for 24 h before whole-cell lysates were analyzed for histone acetylation by Western immunoblot.

Table 2. IC_{50}s of MGCD0103, its inactive analogue (compound A) and SAHA *in vitro* in MTT assays using various human cultured cell lines

Cell line	Tissue origin	MTT IC_{50} ± SE (μmol/L)*			
		MGCD0103	Compound A	SAHA	MS-275
HCT116	Colon carcinoma	0.29 ± 0.02	40 ± 5	0.9 ± 0.1	0.75 ± 0.02
HCT15		0.72 ± 0.03	6.4 ± 0.7	2.5 ± 0.4	2.16 ± 0.30
HT29		0.76 ± 0.06	38 ± 5	1.1 ± 0.2	1.89 ± 0.29
DU145	Prostate carcinoma	0.67 ± 0.07	14 ± 2	0.8 ± 0.2	1.26 ± 0.06
MDA-mb231	Breast carcinoma	0.61 ± 0.07	8 ± 1	0.8 ± 0.2	2.73 ± 0.35
T24	Bladder carcinoma	0.66 ± 0.05	30 ± 14	2.3 ± 0.4	1.74 ± 0.16
A549	Non–small cell lung carcinoma	0.9 ± 0.04	21 ± 9	1.3 ± 0.4	7.86 ± 0.32
H1437		1.45 ± 0.21	8.5 ± 0.62	1.38 ± 0.23	0.97 ± 0.17
BxPc3	Pancreatic carcinoma	1.4 ± 0.2	10 ± 0.9	2.3 ± 0.3	3.43 ± 0.50
Jurkat-T	T-cell leukemia	0.09 ± 0.01	>50	0.43 ± 0.07	0.27 ± 0.02
U937	Histiocytic lymphoma	0.11 ± 0.01	4 ± 0.3	0.77 ± 0.14	0.38 ± 0.03
HL60	Promyelocytic leukemia	0.18 ± 0.02	6.6 ± 0.5	1.5 ± 0.3	0.85 ± 0.09
RPMI-8226	B-cell myeloma	0.15 ± 0.02	11 ± 2	0.58 ± 0.04	0.18 ± 0.03
MV-4-11	Myelomonocytic leukemia	0.1 ± 0.01	2.8 ± 0.3	0.2 ± 0.03	0.41 ± 0.04
HMEC	Breast normal epithelial	20 ± 2	15 ± 3	32 ± 4	>25
MRHF	Foreskin fibroblast	15.0 ± 3.3	N.E.	0.4 ± 0.2	>25

Abbreviation: N.E., not evaluated.
*The numbers represent the concentration (μmol/L) that reduced cell numbers to 50% relative to DMSO-treated cells (IC_{50}) ± SE to the mean. All experiments were done at least thrice independently.

48 hours after drug removal followed by a slow reversal. The long-lasting enzyme inhibitory activity was not limited to cancer cells, as we observed a similar effect in human peripheral WBC treated with MGCD0103 *ex vivo*, suggesting that this surrogate tissue may be useful to study the pharmacodynamics of HDAC activity in clinical trials of MGCD0103.[6]

Isotype-Selective HDAC Inhibition Induces Histone Acetylation but Has No Effect on Tubulin Acetylation

HDAC inhibition by MGCD0103 induced histone H3 and H4 acetylation in human cancer T24 cells (Fig. 2D, *lane 1–5*), A549, and HCT116 cells (data not shown) in a dose-dependent manner. Induction of histone acetylation in T24 cancer cells required HDAC inhibitory activity, as the desamino analogue, compound A, did not induce histone hyperacetylation in these cells (Fig. 2D, *lane 6*). The degree of hyperacetylation was greater with MGCD0103 than SAHA at equivalent concentrations (Fig. 2D, *lane 7–9*). As further confirmation of isotype selectivity, tubulin acetylation, an effect attributed to HDAC6 inhibition, was evaluated by Western blot or ELISA. Tubulin acetylation was not induced by MGCD0103 at concentrations of up to 25 μmol/L in either T24 cells or A549 cells (data not shown).

Antiproliferative Activity of MGCD0103 Is Selective to Cancer Cells and Requires Its HDAC Inhibitory Activity

As shown in Table 2, MGCD0103 exhibited a dose-dependent antiproliferative activity against a broad spectrum of human cancer cell lines from a variety of tissue origins, including solid tumor and hematologic malignancies. The antiproliferative activity of MGCD0103 required its HDAC enzyme inhibitory activity, as compound A, which had no inhibitory activity toward HDAC1/HDAC2, did not exhibit a significant antiproliferative effect. In contrast, MGCD0103 did not have antiproliferative activity in human normal cells, such as HMEC cells or MRHF cells (Table 2). We also observed that MGCD0103 exhibited a more potent antiproliferative effect than SAHA or MS-275 in various human cancer cell lines we tested (Table 2). MGCD0103 activity was at least 3-fold more potent than SAHA in HCT116, HCT15, T24, Jurkat-T, U937, HL60, and RPMI-8226 cell lines, and at least 3-fold more potent than MS-275 in HCT15, MDA-mb231, A549, Jurkat-T, MV-4-11 cell lines. Unlike both MGCD0103 and MS-275, SAHA had a strong antiproliferative activity in normal human fibroblast MRHF cells.

Induction of Cell Cycle Arrest and p21 Expression in Human Cancer Cell Lines *In vitro*

Cell cycle profiles of human cancer cell lines, including HCT116 (Fig. 3A), A549, T24 (data not shown), and normal HMEC cells (Fig. 3B) treated with MGCD0103 *in vitro* were analyzed by flow cytometry. In HCT116 cells (Fig. 3A), MGCD0103 induced a significant S-phase depletion and both G_1 and G_2-M accumulation. Sub-G_1 accumulation was also induced in HCT116 cells in a dose-dependent manner. In contrast, cell cycle profiles of HMEC cells were unchanged at 1 μmol/L and minimally affected by MGCD0103 at a high concentration (10 μmol/L; Fig. 3B).

We also examined the effect of MGCD0103 on the protein expression of $p21^{cip/waf1}$, a cyclin-dependent kinase inhibitor, in human cancer cells. Induction of $p21^{cip/waf1}$ expression in HCT116 cancer cells (Fig. 3C, *lane 1–5*) was

[6] Bonfils C., Kalita A., Dubay M., Siu L., Carducci M.A., Reid G., Martell R., Besterman J.M., Li Z. Evaluation of the pharmacodynamic effects of MGCD0103 from preclinical models to human, using a novel HDAC enzyme assay. *Clin Cancer Res* (in press).

dose-dependent and required HDAC inhibitory activity. Compound A had no effect (Fig. 3C, *lane 6*). Induction of $p21^{cip/waf1}$ expression was not limited to a particular cancer cell line or to the p53 status in these cell lines, because we found MGCD0103 also induced p21 expression at the protein level in a dose-dependent manner in A549 cells (with wild-type p53) and p53-null T24 cells and U937 lymphoma cell lines (data not shown).

Induction of Apoptosis in Human Cancer Cells by MGCD0103 *In vitro*

To investigate whether MGCD0103 induces apoptosis in cancer cells and whether the induced apoptosis was caspase-dependent, we analyzed PARP cleavage in HCT116 cells using an antibody which specifically recognized a caspase-specific cleaved PARP fragment. As shown in Fig. 3D, we observed caspase-specific degradation of PARP by MGCD0103 in a dose-dependent manner in HCT116 cancer cells. Induction of apoptosis by MGCD0103 was also observed in other cancer cell lines, including A549 and T24, but not in normal human epithelial HMEC cells as determined by mononucleosome release in cells (data not shown).

Broad Spectrum Antitumor Activity in Human Tumor Xenograft Models and Induction of Histone Acetylation in Tumors *In vivo*

To assess the ability of MGCD0103 to inhibit tumor growth *in vivo*, we examined its effect in s.c. implanted human tumors in nude mice. As shown in Fig. 4A, p.o. administration of MGCD0103 (2HBr salt) significantly reduced growth of implanted advanced A549 tumors in nude mice in a dose-dependent manner after 13 days of daily administration. MGCD0103 (170 mg/kg for 2HBr salt, corresponding to 120 mg/kg of free base) significantly blocked growth of tumors compared with vehicle treatment alone ($P < 0.05$ in post-ANOVA Dunnett's test) with no change in body weight. In addition, MGCD0103 did not reduce WBC counts and was well tolerated. In the same experiment, we analyzed antitumor activity of SAHA by daily i.p. administration at 90 mg/kg, which is close to its toxic dose in mice (100 mg/kg). Under those experimental conditions, SAHA did not have any antitumor activity in A549 NSCLC.

The plasma concentrations of MGCD0103 and SAHA were analyzed after the last dose at the end of the study. As shown in Fig. 4B, time-dependent and dose-dependent plasma accumulation of MGCD0103 had been observed. At 4 hours post-dose, the plasma levels of MGCD0103 remained above the IC_{50} against HDAC1 and HDAC2 *in vitro* (0.1–0.3 μmol/L). Antitumor efficacy of MGCD0103 correlated with plasma exposure of MGCD0103 in mice *in vivo*. Because SAHA was given i.p. rather than p.o., the initial time point for drug analysis was 15 minutes only after the last dose, whereas the analysis for MGCD0103 was started 1 hour after p.o. administration. Although the time points are not identical, the initial plasma concentration of SAHA was comparable with that of MGCD0103, but decreased much faster.

MGCD0103 was also orally active in many other human tumor xenograft models, such as NSCLC H1437 (Fig. 4C), prostate tumor Du145, and colon tumors (Colo205 and HCT116; see Supplementary materials). As shown in Fig. 4C, MGCD0103 at 80 mg/kg (free base) almost completely blocked the growth of H1437 tumors after 13 days of daily p.o. administration (*t* test, $P = 0.007$) with no reduction of body weight in animals.

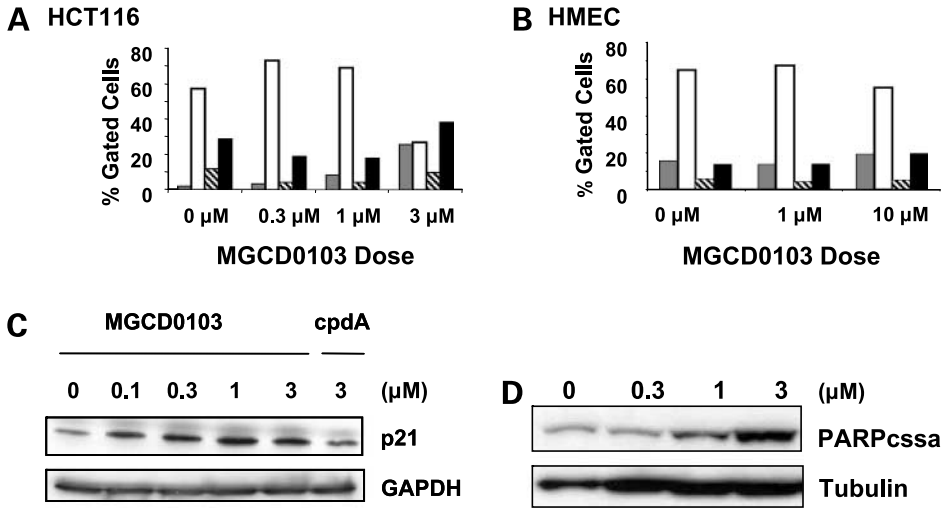

Figure 3. Cell cycle profiles of human cancer HCT116 cells (**A**) and normal HMEC cells (**B**) treated for 16 h with MGCD0103 (in final 1% DMSO) at different doses: sub-G_1 (*gray columns*), G_1 (*white column*), S (*striped columns*), and G_2-M (*black columns*). **C,** dose-dependent induction of $p21^{WAF/Cip1}$ protein *in vitro* in HCT116 cells by 24-h treatment with MGCD0103 or compound A. Whole-cell lysates were immunoblotted with anti-$p21^{WAF/Cip1}$ antibody (Transduction Laboratories). Protein levels of glyceraldehyde-3-phosphate dehydrogenase (*GAPDH*) in the same samples were used to monitor loading. **D,** dose-dependent induction of caspase-specific cleavage of PARP in HCT116 cells by MGCD0103 after 24-h treatment. PARP cleavage was detected by immunoblotting using an antibody specific to a caspase cleavage product of PARP (*PARPcssa*). The protein levels of tubulin in the same samples were used to monitor loading.

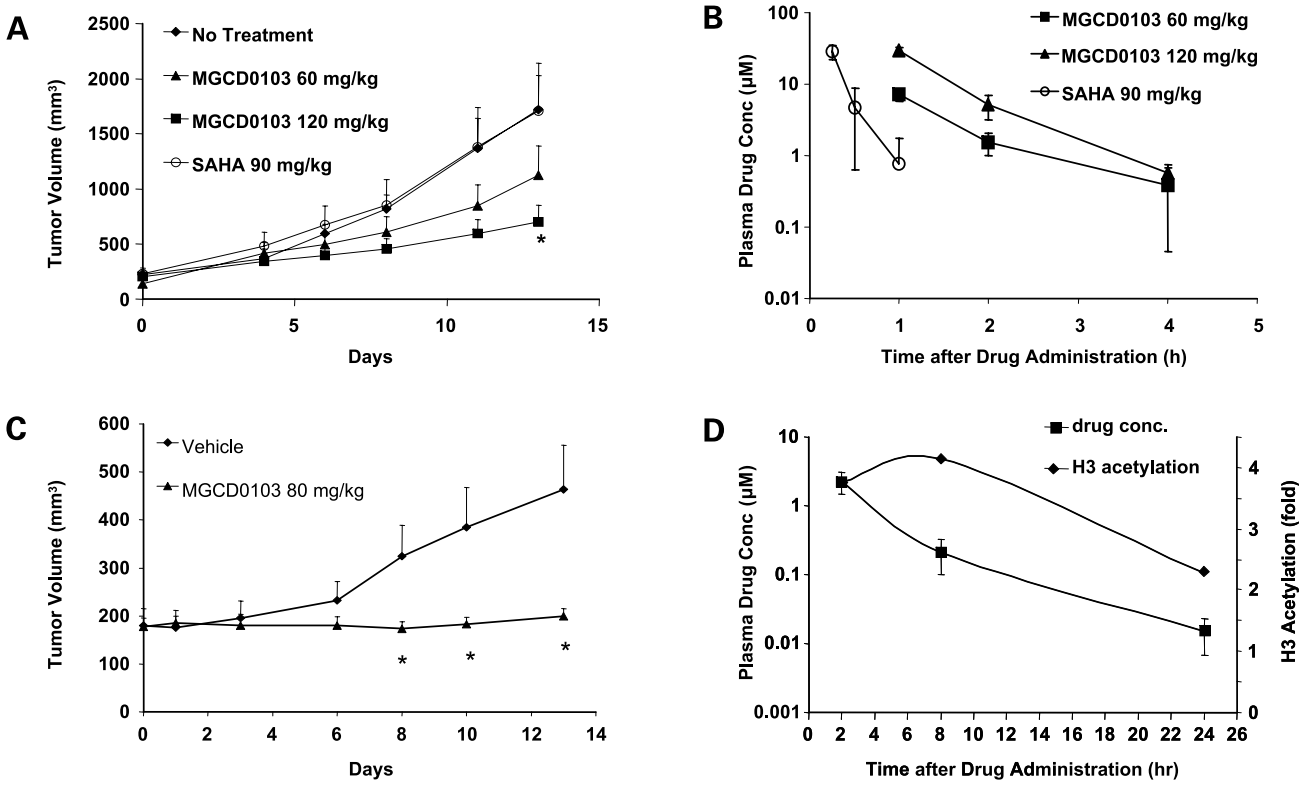

Figure 4. *In vivo* antitumor efficacy and pharmacokinetic and pharmacodynamic features of MGCD0103. **A,** tumor volumes of A549 human tumors implanted in nude mice treated daily with p.o. administration of MGCD0103 (2HBr salt) in saline acidified with 0.1 N HCl at 85 mg/kg 2HBr salt (equal to 60 mg/kg free base; *triangle*), at 170 mg/kg 2HBr salt (equal to 120 mg/kg free base; *square*), with i.p. administration of SAHA at 90 mg/kg in DMSO (*open circles*), or no treatment (*diamond*). The maximum volume for daily administration was 200 μL per animal for p.o. dosing and 20 μL for i.p. Each group consisted in six mice, each implanted with one tumor on each flank. *Error bars,* SE; *star,* statistical significance (post-ANOVA Dunnett's test at 0.05) between the group treated with MGCD0103 (120 mg/kg free base) and the no treatment group. **B,** plasma concentration of MGCD0103 in treated mice in **A** after the last dose; p.o. administration of MGCD0103 at 60 mg/kg free base (*square*) or 120 mg/kg free base (*triangle*); i.p. administration of SAHA at 90 mg/kg (*open circles*). *Error bars,* SD of the average value for each data point. **C,** inhibition of tumor growth of H1437 tumors implanted in nude mice after daily p.o. administration of MGCD0103 (120 mg/kg of 2HBr salt, corresponding to 80 mg/kg of free base). Tumor volume changes significant when compared with the vehicle (PEG 400/0.2 mol/L HCl saline, 40:60) are represented with stars. **D,** time-dependent induction of histone H3 acetylation in implanted HCT116 tumors and time-dependent kinetics of MGCD0103 in plasma of treated mice (90 mg/kg group in **C**). H3 acetylation fold induction in tumors as measured by Western immunoblotting (*right axis*; *diamonds*) and plasma drug concentration (*left axis*; *squares*) *in vivo* in mice.

To correlate the pharmacodynamics with pharmacokinetics of MGCD0103, we analyzed the kinetics of histone acetylation from HCT116 tumors and plasma drug exposure at the end of 18 days of treatment (90 mg/kg group; see Supplementary material). As shown in Fig. 4D, MGCD0103 was detectable in plasma 24 h after dosing and the concentration was at or above the IC_{50} against the HDAC1 and HDAC2 enzymes *in vitro* (Table 1) for the first 8 hours. Induction of histone H3 acetylation in tumors was observed for at least 24 hours post-dose, with a maximal induction from 2 to 8 hours post-dose. Histone H3 acetylation was still higher than baseline at 24 hours post-dose, a time point when the drug exposure is minimal in plasma. Thus, the pharmacodynamics of MGCD0103 persisted beyond the detectable plasma levels.

Discussion

Our studies using antisense to HDAC1, HDAC2, HDAC3, and HDAC6 suggest that HDAC1 is the major isotype, among the four isotypes tested, associated with growth arrest and apoptosis of human cancer cell lines. These effects were selective to cancer cells as they were not observed in a normal mammary epithelial cell line. This is consistent with other findings that HDAC1 is essential for proliferation of human cancer cells (41–43) but less consistent with other reports (41, 44) supporting the roles of HDAC2 or HDAC3. The observed discrepancy between our observations and other reports on the function of HDAC2 and HDAC3 in cancer (41, 44) may be due to varying HDAC isotype expression levels and pathways in different cancer cell lines. Nevertheless, it is clear that the inhibition of HDAC1 is a key objective that we and others have identified for human anticancer therapeutics.

Guided by these target validation results, we designed and synthesized a novel isotype-selective HDAC inhibitor, MGCD0103. Our results show that MGCD0103, a novel aminophenylbenzamide, is an isotype-selective HDAC inhibitor, which primarily targets human HDAC1 and HDAC2 enzymes with weaker inhibition of HDAC3 and

HDAC11, and does not inhibit HDAC4, HDAC5, HDAC6, HDAC7, or HDAC8. Consistent with its isotype selectivity, MGCD0103 inhibited only 75% to 80% of total HDAC activity in various intact human cells compared with an inhibition of 100% and >90% activity respectively by the hydroxamic acid inhibitors NVP-LAQ824 and SAHA. These findings suggest that in intact cells MGCD0103 has a narrower target spectrum compared with the nonselective inhibitors NVP-LAQ824 and SAHA.

Vorinostat (SAHA) and other HDAC inhibitors in clinical development, such as LBH589 and PXD101, target both class I and class II HDAC enzymes. Although our data show that MGCD0103 and SAHA have similar spectra of activity in human cancer cell lines *in vitro*, including in human A549 cancer cells, MGCD0103 was more active than SAHA under our experimental conditions in an A549 tumor xenograft model, despite a similar initial drug concentration in plasma (Fig. 4B). SAHA has been previously reported to be very active in a CWR22 prostate cancer xenograft model (45); the discrepancy with our results might come from using different conditions and tumor types. Nonetheless, our data suggest that antitumor efficacy does not necessitate a nonselective inhibition of HDAC isoforms. Instead, selective inhibition of a few HDAC isotypes by MGCD0103 is sufficient for antiproliferative activity *in vitro* and *in vivo*. A recent report has also confirmed the approach (46). The clinical outcomes with MGCD0103 and other selective inhibitors will ultimately provide insight as to whether isotype-selective inhibitors have advantages over nonselective inhibitors in cancer patients.

MGCD0103 is a nonhydroxamate inhibitor; its warhead for HDAC inhibition is a benzamide group rather than the hydroxamate group present in SAHA, LBH589, and PXD101. MGCD0103 may have a different mechanism of enzyme inhibition than that of hydroxamate-based inhibitors, possibly through different mechanism of Zn^{2+} chelation. We built a homology model of HDAC1 around the published coordinates of HDLP (ref. 47; data not shown). Our model shows that the carbonyl-oxygen and the ortho-NH_2 groups directly interact with the Zn^{2+} ion. Besides, these two groups also form potential hydrogen bonds with the side chains of several key amino acids in the active site. The aniline ring is partially filling the 14 Å hydrophobic cavity adjacent to the catalytic site contributing with potential beneficial interactions. Similar binding mode of MS-275 in a human HDAC1 homology model has been recently disclosed (48). Our present study also confirms that the free amino group of benzamide of MGCD0103 is essential for its inhibitory activity on HDAC enzymes both *in vitro* with the recombinant enzyme and in whole cells.

MGCD0103 is orally available in mouse, and it also has an extended pharmacodynamic effect *in vitro* and *in vivo*. The HDAC inhibitory activity persists for up to 48 hours posttreatment *in vitro*, and histone acetylation persists for up to 24 hours in mice *in vivo*. The kinetics of the pharmacodynamic activities of MGCD0103 suggested that an intermittent dosing schedule may be effective. Indeed, several dosing regimens of MGCD0103 have been evaluated in the clinic, and oral MGCD0103 is now in multiple phase 2 clinical trials on both thrice-a-week and twice-a-week schedules. Evidence of single-agent antitumor activity in relapsed or refractory acute myelogenous leukemia or myelodysplastic syndrome (49) and in relapsed or refractory Hodgkin's lymphoma (50) has been observed.

Acknowledgments

We thank other members of HDAC Oncology team from MethylGene, in the present or past, for their contributions toward the discovery of MGCD0103; Drs. Arkadii Vaisburg, Silvana Leit, Stéphane Raeppel, Sylvie Fréchette, Isabelle Paquin, and Frédérick Gaudette from Medicinal Chemistry Department of MethylGene, Inc.; our colleagues from Taiho Pharmaceuticals who provided homology modeling of human HDAC1 and docking of MGCD0103 in the model; our colleagues in MethylGene, Inc., Taiho Pharmaceuticals, and Pharmion Corp. for critical reading of this manuscript, especially Dr. Carla Heise for her constructive suggestions; and Neil Malone, Debbie Evanoff, and Sue Garrett from Pharmion Corporation for editorial help. MGCD0103 is currently in clinical development by the collaboration among MethylGene, Inc., Pharmion Corporation, and Taiho Pharmaceuticals.

References

1. Gray SG, Ekstrom TJ. The human histone deacetylase family. Exp Cell Res 2001;262:75 – 83.

2. Thiagalingam S, Cheng KH, Lee HJ, Mineva N, Thiagalingam A, Ponte JF. Histone deacetylases: unique players in shaping the epigenetic histone code. Ann N Y Acad Sci 2003;983:84 – 100.

3. Denu JM. The Sir 2 family of protein deacetylases. Curr Opin Chem Biol 2005;9:431 – 40.

4. Buck SW, Gallo CM, Smith JS. Diversity in the Sir2 family of protein deacetylases. J Leukoc Biol 2004;75:939 – 50.

5. Taunton J, Hassig CA, Schreiber SL. A mammalian histone deacetylase related to the yeast transcriptional regulator Rpd3p. Science New York N Y 1996;272:408 – 11.

6. Yang WM, Inouye C, Zeng Y, Bearss D, Seto E. Transcriptional repression by YY1 is mediated by interaction with a mammalian homolog of the yeast global regulator RPD3. Proc Natl Acad Sci U S A 1996;93: 12845 – 50.

7. Yang WM, Yao YL, Sun JM, Davie JR, Seto E. Isolation and characterization of cDNAs corresponding to an additional member of the human histone deacetylase gene family. J Biol Chem 1997;272:28001 – 7.

8. Van den Wyngaert I, de Vries W, Kremer A, et al. Cloning and characterization of human histone deacetylase 8. FEBS Lett 2000;478: 77 – 83.

9. Hu E, Chen Z, Fredrickson T, et al. Cloning and characterization of a novel human class I histone deacetylase that functions as a transcription repressor. J Biol Chem 2000;275:15254 – 64.

10. Fischle W, Emiliani S, Hendzel MJ, et al. A new family of human histone deacetylases related to *Saccharomyces cerevisiae* HDA1p. J Biol Chem 1999;274:11713 – 20.

11. Grozinger CM, Hassig CA, Schreiber SL. Three proteins define a class of human histone deacetylases related to yeast Hda1p. Proc Natl Acad Sci U S A 1999;96:4868 – 73.

12. Wang AH, Bertos NR, Vezmar M, et al. HDAC4, a human histone deacetylase related to yeast HDA1, is a transcriptional corepressor. Mol Cell Biol 1999;19:7816 – 27.

13. Kao HY, Downes M, Ordentlich P, Evans RM. Isolation of a novel histone deacetylase reveals that class I and class II deacetylases promote SMRT-mediated repression. Genes Dev 2000;14:55 – 66.

14. Zhou X, Marks PA, Rifkind RA, Richon VM. Cloning and characterization of a histone deacetylase, HDAC9. Proc Natl Acad Sci U S A 2001; 98:10572 – 7.

15. Kao HY, Lee CH, Komarov A, Han CC, Evans RM. Isolation and characterization of mammalian HDAC10, a novel histone deacetylase. J Biol Chem 2002;277:187 – 93.

16. Gao L, Cueto MA, Asselbergs F, Atadja P. Cloning and functional

characterization of HDAC11, a novel member of the human histone deacetylase family. J Biol Chem 2002;277:25748 – 55.

17. Fraga MF, Ballestar E, Villar-Garea A, et al. Loss of acetylation at Lys16 and trimethylation at Lys20 of histone H4 is a common hallmark of human cancer. Nat Genet 2005;37:391 – 400.

18. Choi JH, Kwon HJ, Yoon BI, et al. Expression profile of histone deacetylase 1 in gastric cancer tissues. Jpn J Cancer Res 2001;92:1300 – 4.

19. Halkidou K, Gaughan L, Cook S, Leung HY, Neal DE, Robson CN. Upregulation and nuclear recruitment of HDAC1 in hormone refractory prostate cancer. Prostate 2004;59:177 – 89.

20. Kawai H, Li H, Avraham S, Jiang S, Avraham HK. Overexpression of histone deacetylase HDAC1 modulates breast cancer progression by negative regulation of estrogen receptor α. Int J Cancer 2003;107: 353 – 8.

21. Wilson AJ, Byun DS, Popova N, et al. Histone deacetylase 3 (HDAC3) and other class I HDACs regulate colon cell maturation and p21 expression and are deregulated in human colon cancer. J Biol Chem 2006;281: 13548 – 58.

22. Zhu P, Martin E, Mengwasser J, Schlag P, Janssen KP, Gottlicher M. Induction of HDAC2 expression upon loss of APC in colorectal tumorigenesis. Cancer Cell 2004;5:455 – 63.

23. Melnick A, Licht JD. Histone deacetylases as therapeutic targets in hematologic malignancies. Curr Opin Hematol 2002;9:322 – 32.

24. Altucci L, Clarke N, Nebbioso A, Scognamiglio A, Gronemeyer H. Acute myeloid leukemia: therapeutic impact of epigenetic drugs. Int J Biochem Cell Biol 2005;37:1752 – 62.

25. Johnstone RW. Histone-deacetylase inhibitors: novel drugs for the treatment of cancer. Nat Rev 2002;1:287 – 99.

26. Marks P, Rifkind RA, Richon VM, Breslow R, Miller T, Kelly WK. Histone deacetylases and cancer: causes and therapies. Nat Rev Cancer 2001;1:194 – 202.

27. Monneret C. Histone deacetylase inhibitors for epigenetic therapy of cancer. Anticancer Drugs 2007;18:363 – 70.

28. Bolden JE, Peart MJ, Johnstone RW. Anticancer activities of histone—deacetylase inhibitors. Nat Rev 2006;5:769 – 84.

29. Kelly WK, Marks PA. Drug insight: histone deacetylase inhibitors—development of the new targeted anticancer agent suberoylanilide hydroxamic acid. Nat Clin Pract 2005;2:150 – 7.

30. Minucci S, Pelicci PG. Histone deacetylase inhibitors and the promise of epigenetic (and more) treatments for cancer. Nat Rev Cancer 2006;6: 38 – 51.

31. Xu WS, Parmigiani RB, Marks PA. Histone deacetylase inhibitors: molecular mechanisms of action. Oncogene 2007;26:5541 – 52.

32. Richon VM, Emiliani S, Verdin E, et al. A class of hybrid polar inducers of transformed cell differentiation inhibits histone deacetylases. Proc Natl Acad Sci U S A 1998;95:3003 – 7.

33. George P, Bali P, Annavarapu S, et al. Combination of the histone deacetylase inhibitor LBH589 and the hsp90 inhibitor 17-AAG is highly active against human CML-BC cells and AML cells with activating mutation of FLT-3. Blood 2005;105:1768 – 76.

34. Plumb JA, Finn PW, Williams RJ, et al. Pharmacodynamic response and inhibition of growth of human tumor xenografts by the novel histone deacetylase inhibitor PXD101. Mol Cancer Ther 2003;2:721 – 8.

35. Furumai R, Matsuyama A, Kobashi N, et al. FK228 (depsipeptide) as a natural prodrug that inhibits class I histone deacetylases. Cancer Res 2002;62:4916 – 21.

36. Marks PA. Discovery and development of SAHA as an anticancer agent. Oncogene 2007;26:1351 – 6.

37. Saito A, Yamashita T, Mariko Y, et al. A synthetic inhibitor of histone deacetylase, MS-27 – 275, with marked *in vivo* antitumor activity against human tumors. Proc Natl Acad Sci U S A 1999;96:4592 – 7.

38. Hu E, Dul E, Sung CM, et al. Identification of novel isoform-selective inhibitors within class I histone deacetylases. J Pharmacol Exp Ther 2003; 307:720 – 8.

39. Karagiannis TC, El-Osta A. Will broad-spectrum histone deacetylase inhibitors be superseded by more specific compounds? Leukemia 2007; 21:61 – 5.

40. Zweidler A. Resolution of histones by polyacrylamide gel electrophoresis in presence of nonionic detergents. Methods Cell Biol 1978;17:223 – 33.

41. Glaser KB, Li J, Staver MJ, Wei RQ, Albert DH, Davidsen SK. Role of class I and class II histone deacetylases in carcinoma cells using siRNA. Biochem Biophys Res Commun 2003;310:529 – 36.

42. Lagger G, O'Carroll D, Rembold M, et al. Essential function of histone deacetylase 1 in proliferation control and CDK inhibitor repression. EMBO J 2002;21:2672 – 81.

43. Senese S, Zaragoza K, Minardi S, et al. Role for histone deacetylase 1 in human tumor cell proliferation. Mol Cell Biol 2007;27:4784 – 95.

44. Huang BH, Laban M, Leung CH, et al. Inhibition of histone deacetylase 2 increases apoptosis and $p21^{Cip1/WAF1}$ expression, independent of histone deacetylase 1. Cell Death Differ 2005;12:395 – 404.

45. Butler LM, Agus DB, Scher HI, et al. Suberoylanilide hydroxamic acid, an inhibitor of histone deacetylase, suppresses the growth of prostate cancer cells *in vitro* and *in vivo*. Cancer Res 2000;60:5165 – 70.

46. Beckers T, Burkhardt C, Wieland H, et al. Distinct pharmacological properties of second generation HDAC inhibitors with the benzamide or hydroxamate head group. Int J Cancer 2007;121:1138 – 48.

47. Finnin MS, Donigian JR, Cohen A, et al. Structures of a histone deacetylase homologue bound to the TSA and SAHA inhibitors. Nature 1999;401:188 – 93.

48. Moradei OM, Mallais TC, Frechette S, et al. Novel aminophenyl benzamide-type histone deacetylase inhibitors with enhanced potency and selectivity. J Med Chem 2007;50:5543 – 6.

49. Garcia-Manero G, Minden M, Estrov Z, et al. Clinical activity and safety of the histone deacetylase inhibitor MGCD0103: results of a phase I study in patients with leukemia or myelodysplastic syndromes (MDS). 2006 ASCO Annual Meeting. J Clin Oncol 2006;24:6500.

50. Younes A, Fanale M, Pro B, et al. A phase II study of a novel oral isotype-selective histone deacetylase (HDAC) inhibitor in patients with relapsed or refractory Hodgkin lymphoma. 2007 ASCO Annual Meeting. J Clin Oncol 2007;25:8000.